JOURNAL OF VIROLOGY, Dec. 1997, p. 9743–9752 Vol. 71, No. 12
0022-538X/97/$04.00+0

Dissecting the Roles of VP0 Cleavage and RNA Packaging in Picornavirus Capsid Stabilization: the Structure of Empty Capsids of Foot-and-Mouth Disease Virus

STEPHEN CURRY,[1]† ELIZABETH FRY,[2] WENDY BLAKEMORE,[1] ROBIN ABU-GHAZALEH,[1] TERRY JACKSON,[1] ANDREW KING,[1] SUSAN LEA,[2] JOHN NEWMAN,[1] AND DAVID STUART[2,3]*

Pirbright Laboratory, Institute for Animal Health, Pirbright, Surrey GU24 0NF,[1] Laboratory of Molecular Biophysics, Oxford University, Oxford OX1 3QU,[2] and Oxford Centre for Molecular Sciences, New Chemistry Laboratory, Oxford OX1 3QT,[3] United Kingdom

Received 13 May 1997/Accepted 18 August 1997

Empty capsids of foot-and-mouth disease virus (FMDV) type A22 Iraq 24/64, whose structure has been solved by X-ray crystallography, are unusual for picornaviruses since they contain VP2 and VP4, the cleavage products of the protein precursor VP0. Both the N terminus of VP1 and the C terminus of VP4, which pack together close to the icosahedral threefold symmetry axis where three pentamers associate, are more disordered in the empty capsid than they are in the RNA-containing virus. The ordering of these termini in the presence of RNA strengthens interactions within a single protomer and between protomers belonging to different pentamers. The disorder in the FMDV empty capsid forms a subset of that seen in the poliovirus empty capsid, which has VP0 intact. Thus, VP0 cleavage confers stability on the picornavirus capsid over and above that attributable to RNA encapsidation. In both FMDV and poliovirus empty capsids, the internal disordering uncovers a conserved histidine which has been proposed to be involved in the cleavage of VP0. A comparison of the putative active sites in FMDV and poliovirus suggests a structural explanation for the sequence specificity of the cleavage reaction.

Molecular details of the interactions governing assembly and stabilization of a number of different unenveloped icosahedral viruses have previously been elucidated by X-ray crystallography. Plant, insect, and mammalian virus capsids have all been studied at atomic resolution. Of the mammalian viruses investigated, the picornaviruses are perhaps the best-characterized family. Picornaviruses are divided into five major genera, enteroviruses, rhinoviruses, cardioviruses, foot-and-mouth disease viruses (FMDVs), and hepatitis A viruses. Crystal structures have been determined for at least one member of each genus, except for hepatitis A viruses (1, 19, 28, 32), and this abundance of structural information has brought to light both common and diverse features of picornavirus architecture.

The icosahedrally symmetric capsid of each picornavirus is formed by 60 copies of four capsid proteins, VP1 to VP4, and incorporates a single-strand, positive-sense RNA genome. Three of the capsid proteins (VP1 to VP3) have a common core structure, consisting of an eight-stranded β-barrel, with the strands labelled alphabetically from B to I. The main structural differences between picornavirus groups are found in the loops connecting the β-strands (designated by the strands they connect) and in the protein termini. The N termini of VP1 to VP3 are usually confined to the interior of the capsid, whereas the C termini are located on the outside. The whole of VP4 is associated with the interior face of the capsid. VP4 exists initially as an N-terminal extension of VP2 in the precursor VP0. During assembly, five protomers, each containing one copy of VP0, VP1, and VP3, assemble into a pentamer, and 12 pentamers associate with a newly transcribed RNA molecule to form a virus particle. Cleavage of VP0 to VP2 and VP4, which is considered to be autocatalytic, is normally observed only upon encapsidation of RNA in mature virions. A related maturation cleavage is observed during encapsidation by other picornavirus-like viruses of animals, such as nodaviruses (17), but not in any of the picornavirus-like plant viruses. The role of encapsidation-linked cleavage appears to be twofold. First, it stabilizes the mature virion, since the newly created termini of VP2 and VP4 make interactions that reinforce the connection between pentameric subunits (2, 14, 16). Second, a number of previous studies have demonstrated that abrogation of cleavage consistently correlates with loss of infectivity (3, 8, 27), indicating that VP0 cleavage is also crucial for infection. The mechanism for this effect remains unclear (18, 27), but there is evidence to suggest that the release of VP4 from VP0 primes the virus for some step in cell entry (29). A functional parallel between VP0 cleavage in picornaviruses and maturation cleavage of the fusion protein in a number of lipid-enveloped viruses, such as influenza virus and human immunodeficiency virus, has been suggested elsewhere (36).

TABLE 1. Data processing statistics

Parameter (unit)	Value
No. of films	18
No. of images	5
Total no. of reflections	129,230
No. of independent reflections	109,104
Completeness (%)	26.8
R_{merge} (%)[a]	17.7

[a] $R_{merge} = \left(\sum_h \sum_i |(I_h - I_{hi})|\right) / \left(\sum_h \sum_i I_{hi}\right) * 100.$

* Corresponding author. Mailing address: Department of Biochemistry, Laboratory of Molecular Biophysics, University of Oxford, The Rex Richards Building, South Parks Rd., Oxford OX1 3QU, United Kingdom. Phone: (44) 1865 275384. Fax: (44) 1865 275182. E-mail: dave@biop.ox.ac.uk.

† Present address: Biophysics Section, Blackett Laboratory, Imperial College, London SW7 2BZ, United Kingdom.

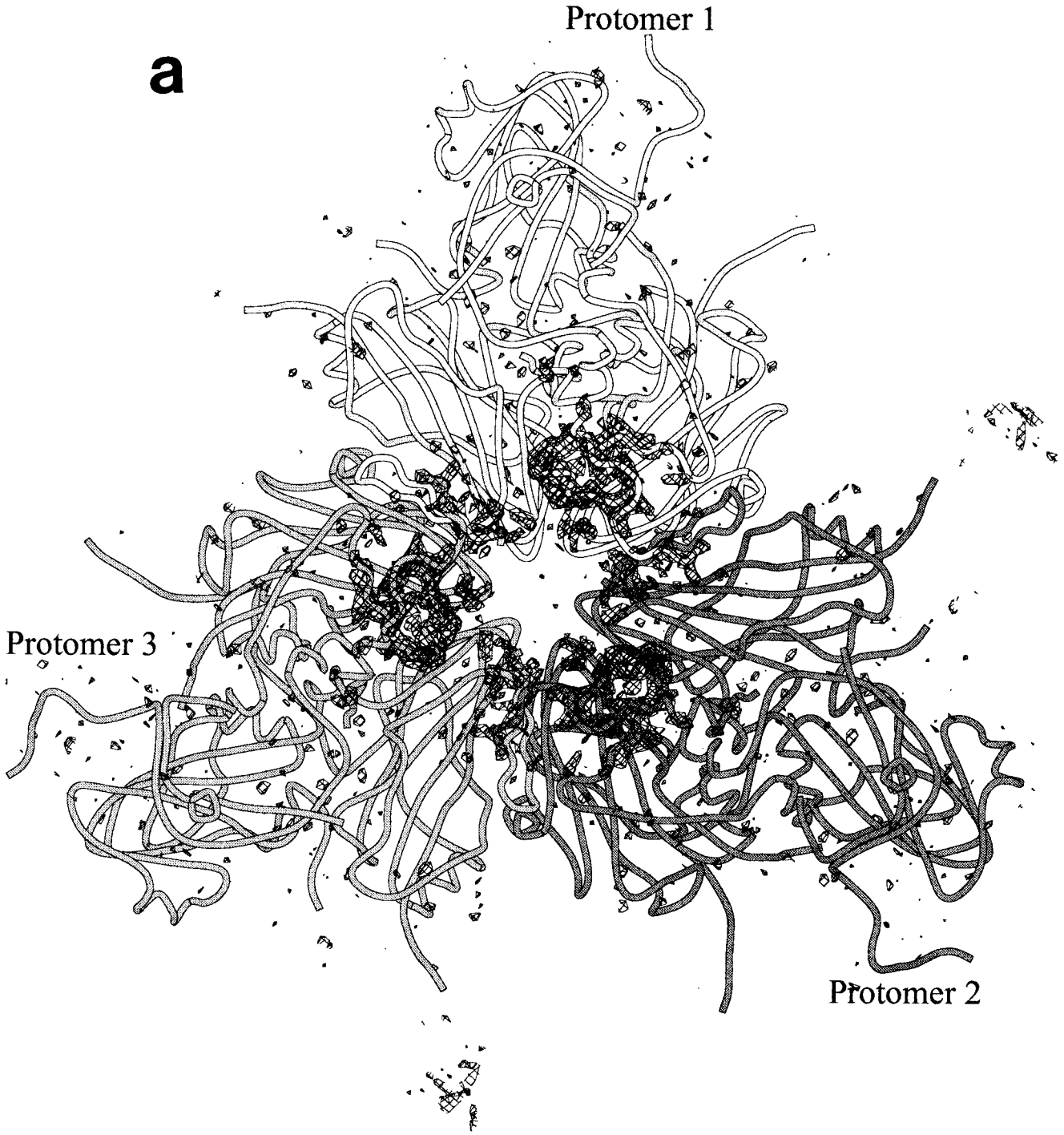

FIG. 1. (a) Difference electron density map illustrating the main differences between the virus and empty capsid of type A22 FMDV. Three protomers related by an icosahedral threefold axis, each belonging to a different pentamer, are shown. The view is onto the interior face of the capsid. A negative-density contour of the electron density map calculated with amplitudes $|F_o^{ec}|$-$|F_o^v|$ indicates the features which are more disordered in the empty capsid than in the virus. (b) Stereo diagram close-up of the view shown in panel a. The most disordered features in FMDV empty capsids are the N terminus of VP1 (VP1-N), the C terminus of VP4 (VP4-C), and portions of the N terminus of VP2 (VP2′-N), all of which are located close to one another in the vicinity of the icosahedral threefold symmetry axis.

Empty capsids lacking the viral RNA are generated during infection by most picornaviruses. Although such capsids have the same total protein content as do normal virions, they are noninfectious and are considered to be either a by-product of infection or a storage form of capsid proteins. Since empty capsids lack viral RNA, maturation cleavage of VP0 does not usually occur. Particles are also generally found to be more thermolabile than is the corresponding virion (12, 31). In order to investigate the role of both RNA encapsidation and VP0 cleavage in the stabilization of picornavirus capsids, we solved the structure of the empty capsid of type A22 Iraq 24/64 FMDV and compared it with the virus. The empty capsids

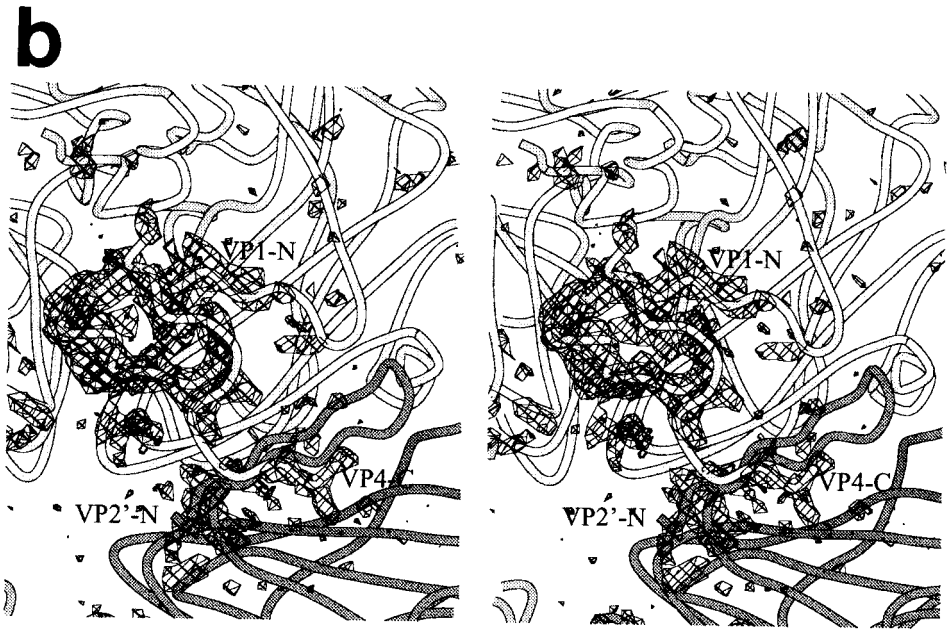

FIG. 1—*Continued.*

purified for this structural study were unusual among picornaviruses in that most of the capsid protein precursor VP0 had been cleaved into VP2 and VP4 (9, 10). Both cleavage products remained associated with the particle; therefore, empty capsids possessed essentially the same polypeptide content as did viruses. A comparison of this empty capsid structure with the virus allowed us to identify those regions within the protein capsid which are affected by the encapsidation of RNA and which may therefore be important for capsid stability in the mature virion. The FMDV empty capsid structure reported here displays a number of key differences from that of the empty capsid of poliovirus (2), in which VP0 remains intact. This allowed us to distinguish the influences of RNA and VP0 cleavage on the capsid architecture. Comparisons between poliovirus and FMDV empty capsids also suggest that the autocatalytic mechanism proposed for VP0 cleavage in poliovirus (2) operates in FMDV.

MATERIALS AND METHODS

Virus growth, purification and crystallization. The virus used in this study was monolayer cell-adapted type A22 Iraq 24/64 FMDV (4). Propagation of this virus and purification and crystallization of virus and empty capsids have previously been described (10).

Data collection and processing. X-ray data collection for parental virus and empty capsids, performed at the SERC Synchrotron Radiation Source, Daresbury, United Kingdom, has previously been described (10). Diffraction data for empty capsids were collected on CEA X-ray film and on a Marresearch Hendrix-Lentfer imaging device on stations 9.6 and 9.5. Film data were processed as described previously (15). Image plate data were measured by using MOSFLM (27a). The data were merged and scaled with ROTAVATA and AGROVATA and postrefined with POSTREF, all programs from the CCP4 package (7). Reflections which were more than 70% recorded were scaled up and treated as fully recorded. The R_{merge} value for empty capsid data was 17.7% (Table 1).

Structure determination. $2F_o^{ec}$-F_o^v and F_o^{ec}-F_o^v maps were calculated with phases derived from the cyclic averaging of the electron density map of the virus (11) (F_o^v and F_o^{ec} are the observed structure factors for the mature virus and empty capsid, respectively). These maps were averaged according to 15-fold noncrystallographic symmetry by using the program GAP (17a). With these maps as guides, the virus model (11) was used as a starting point for model building. The model was subjected to positional and temperature factor (B-factor) refinement with X-PLOR (5). $2F_o^{ec}$-F_c^{ec} and F_o^{ec}-F_c^{ec} maps calculated with amplitudes (F_c^{ec}) and phases from the empty capsid model were used (after 15-fold averaging) to make adjustments and to add 224 water molecules before final positional and B-factor refinement (Table 1).

Residue numbering convention. Residues are numbered according to a four-digit system commonly employed for picornaviruses. The initial digit indicates the virus capsid polypeptide, and the remaining three digits indicate the sequence position within that protein chain. For example, residue 2145 represents amino acid 145 in VP2. In labelling residues within empty capsid structures, in which VP0 is either not cleaved (poliovirus) or is cleaved aberrantly (FMDV), this numbering system is maintained.

Molecular graphics. Model building was performed by using FRODO (20). Figures were prepared by using Bobscript (a version of MOLSCRIPT [24] modified by Robert Esnouf), Raster 3D (8), and Photoshop (Adobe).

Coordinates have been deposited with the Brookhaven Protein Data Bank.

RESULTS

Empty capsids (viral capsids lacking genomic RNA) are a natural product of infection by most picornaviruses. Usually these particles are generated without cleavage of the precursor VP0 into VP2 and VP4 (33), an event normally associated with RNA encapsidation. However, the type A FMDV empty capsids prepared for this crystallographic study were found to contain relatively low amounts of intact VP0. Typically around 40 of 60 possible VP0 molecules per capsid were found to be cleaved to VP2 and VP4, both of which remained associated with the particle (9). Cleavage of VP0 appeared to continue in purified empty capsids with a half-life of about 3 weeks at room temperature (the temperature at which crystallization was performed) so that in crystals used for data collection, the VP0 content was reduced further. The possible reasons for this observation were investigated previously (9), but the mechanism remains a puzzle.

Type A22 FMDV empty capsids crystallized isomorphously with the virus (in space group I222 with the following cell dimensions: a = 328.2 Å, b = 341.2 Å, and c = 363.75 Å) under similar crystal growth conditions (10). An electron density difference map, calculated with amplitudes $|F_o^v|$-$|F_o^{ec}|$ and phases derived from the cyclic averaging of the electron density map of the virus (11), illustrated the principal changes between the virus and empty capsid structures (Fig. 1). The map shows that there are no differences between the virus and empty capsid on

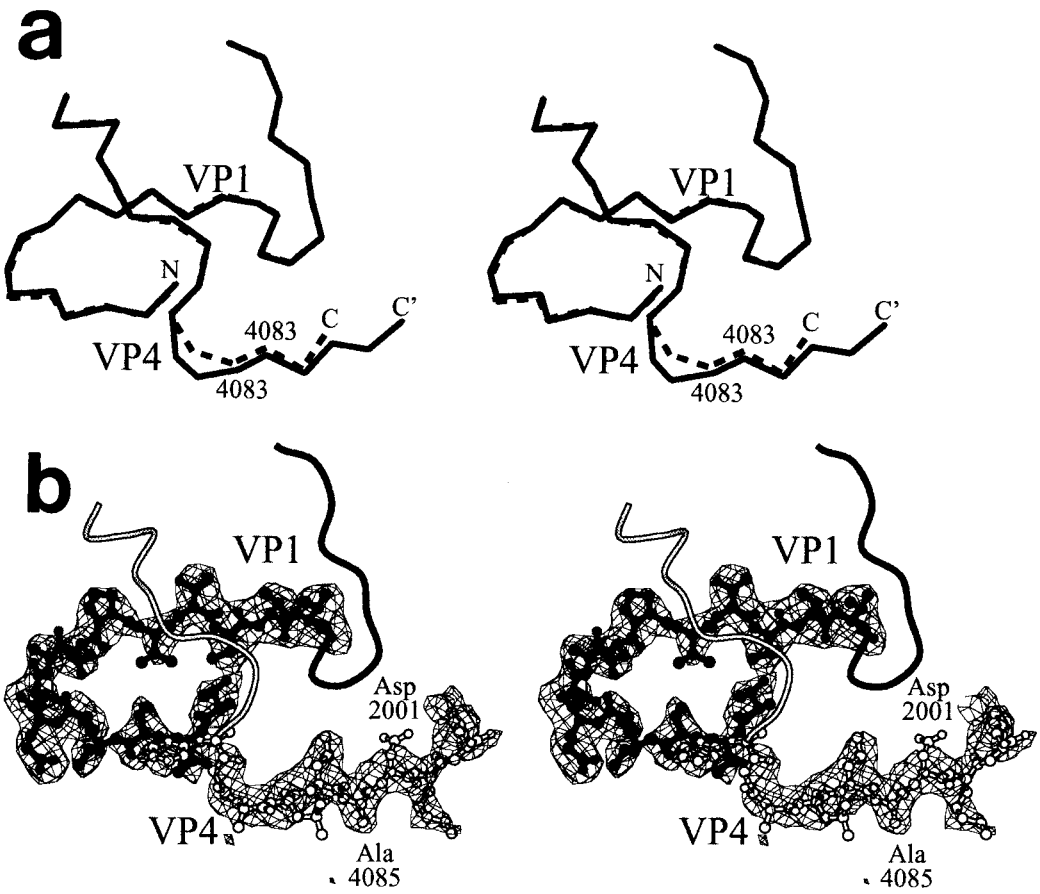

FIG. 2. Model built for the N terminus of VP1 and the C terminus of VP4 in the empty capsid. (a) Apart from the increased disordering of the N terminus of VP1 and the C terminus of VP4 in the empty capsid, the major difference between the virus (dotted lines) and empty capsid (solid lines) lies in the C terminus of VP4. This is 3 residues longer in the empty capsid, extending to 88 rather than 85 amino acids and adopting a slightly wider turn at residue 81. Thus, the positions of residues 4082 to 4084 in the virus are occupied by residues 4083 to 4085 in the empty capsid. (b) The omit map was generated with amplitudes $|F_o^{ec}|-|F_c^{ec}|$ and phases calculated from a model in which the first 15 residues of VP1 and the last 8 residues of VP4 were omitted. These residues are represented as a ball and stick. VP1 is shown in black, and VP4 is shown in white. Residues Ala 4085 and Asp 2001, which are normally separated by the cleavage of VP0, are indicated.

the exterior surface of the particle. The most significant differences are negative-density features confined to the interior of the capsid close to the threefold axis where three pentameric subunits associate (Fig. 1). These indicate that a number of the termini of the capsid proteins close to the threefold axis are significantly more disordered in the empty capsid than they are in the virion. In particular, both the C terminus of VP4 (residues 4067 to 4085) and the N terminus of VP1 (residues 1001 to 1026), which packs underneath it, are more disordered in the empty capsid (the most significant digit of the residue label indicates the capsid protein to which the amino acid belongs, and the remaining three digits give the position within that polypeptide chain [see Materials and Methods]). The disordering of the C terminus of VP4 is most likely due to the absence of RNA rather than to the adoption of different conformations by cleaved and uncleaved VP0; because of the progressive nature of VP0 cleavage, it is unlikely that more than 5% of VP0 remained uncleaved when crystals of FMDV empty capsids were used for X-ray diffraction data collection. To a lesser degree, residues 3153 and 3154 in VP3, which lie directly below the N terminus of VP1, also appear to be more disordered in the empty capsid. Directly underneath the C terminus of VP4 lie residues 2012 to 2028 from the N-terminal portion of VP2 from a protomer related by threefold icosahedral symmetry. The difference density suggests that portions of this N terminus (residues 2013 to 2015 and 2024 to 2028) are less well ordered in the empty capsid (residues 2001 to 2011 of VP2 are not visible in either the virus or empty capsid structure). All other internal features are the same for virus and empty capsid, suggesting that except for the termini noted above, there are no icosahedrally symmetric perturbations of the protein capsid due to RNA encapsidation.

An atomic model for the FMDV empty capsid was built into a $2F_o^{ec}-F_c^{ec}$ electron density map (calculated with phases refined by noncrystallographic symmetry averaging). This model, comprising 5,200 nonhydrogen atoms (with no residues in the disallowed regions of a Ramachandran plot), was refined to an R factor of 20.3% for 109,104 unique reflections (for details, see Materials and Methods). The model is indistinguishable from that of the virus structure, except for those segments associated with negative density in the difference map. Although density in the $2F_o^{ec}-F_c^{ec}$ map corresponding to the N terminus of VP1 and the C terminus of VP4 was observed only at low contour levels, it was still possible to construct a model for these portions of the polypeptide chains. The model suggests that the conformation of the N terminus of VP1 in the empty capsid is essentially the same as that observed in the mature virus. However, the density for the C terminus of VP4 indicated that there

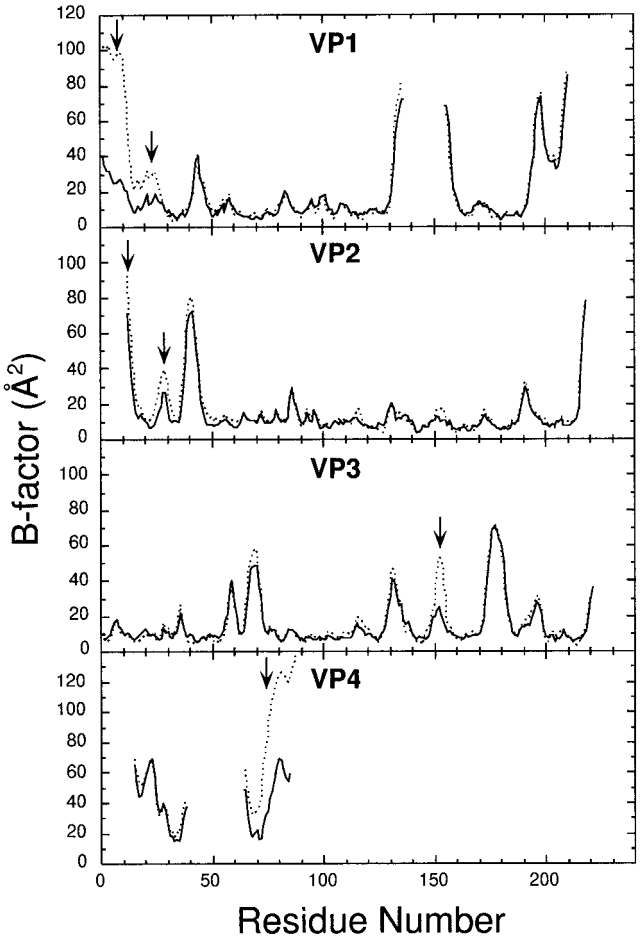

FIG. 3. B factor plots for the capsid proteins of the virus (solid line) and empty capsids (dotted lines) of type A22 FMDV. The plots show the B factor of the C_α atoms as a function of residue number for VP1, VP2, VP3, and VP4. Features which are significantly more disordered in the empty capsid are indicated by arrows.

were small but significant differences with the virus in this region. The model for the C terminus of VP4 built into this density differs from the virus in two respects (Fig. 2). Residues 4080 to 4082 adopt a wider turn in the empty capsid than they do in the virus, and this results in a shift of register in the downstream amino acids between the virus and empty capsid. Thus, residues 4083 to 4085 in the empty capsid occupy the positions of residues 4082 to 4084 in the mature virus (Fig. 2a). Moreover, the density supports the inclusion of three additional residues immediately beyond the expected C-terminal residue of VP4 (Ala 4085). Although it is weak, the density for these additional residues is plausibly accounted for by the sequence, Asp-Lys-Lys, which follows the scissile bond in VP0 that separates VP4 and VP2; in the mature virus, these are residues 2001 to 2003 of VP2. The density stops abruptly after Lys 2003, suggesting that VP0 in type A22 FMDV empty capsids is aberrantly cleaved. The density corresponding to these additional residues at the C terminus of VP4 has not previously been observed in electron density maps for mature virions of three FMDV serotypes (1, 11, 25, 26). The calculation of an F_o^{ec}-F_c^{ec} omit map for the empty capsid, with residues 1001 to 1015, 4080 to 4085, and 2001 to 2003 absent from the phasing model, supported the model interpretation described above (Fig. 2b). Attempts to confirm this interpretation by mass spectrometry analysis failed due to the stringent physical treatment required to remove particles from the Pirbright laboratory (1a). Therefore, biochemical confirmation of the presence of additional residues at the C terminus of VP4 in the empty capsid is still required.

The mechanism that gives rise to the apparently aberrant cleavage in empty capsids is not known. It may arise from a variant of the autocatalytic mechanism thought to be responsible for the normal process of VP4 cleavage in picornaviruses. However, another possibility is that the cleavage is due to either FMDV L or 3C protease, perhaps by encapsidation of the enzyme in the empty capsid. The L protease, which is unique to the aphthovirus genus of picornaviruses and cleaves at Lys-Gly or Gly-Arg junctions (22), may be able to cleave the Lys 2003-Thr 2004 junction in VP0, thus giving rise to the extended VP4 peptide observed in the empty capsid structure. The 3C protease, which normally cleaves at Gln-Thr, Gln-Leu, Gln-Ile, Glu-Thr, Glu-Gly, or Glu-Ser junctions and has also previously been reported to cleave Lys-Ile junctions (35), may also be responsible for the Lys-Thr cleavage indicated by the FMDV empty capsid structure.

Whatever the precise reason for the apparently unusual VP0 cleavage, it is clear that the C terminus of VP4 and the N terminus of VP1 in FMDV empty capsids, when they are ordered, adopt conformations which are similar to those observed in the mature virus. The most important structural change in these features in the absence of packaged RNA is that they become significantly more disordered. This is represented in the model for empty capsids by a dramatic rise in the B factors associated with the atoms in these termini. The B factors, parameters used to characterize the vibrations of atoms in the model about their mean positions, were 60 to 70 Å^2 higher for the N terminus of VP1 and the C terminus of VP4 in the empty capsid (Fig. 3). Portions of the N terminus of VP2 and residues 3152 to 3154 in VP3, which pack against these termini (and were associated with negative density in the difference map), also displayed elevated B factors in the empty capsid model. Elsewhere in the capsid, there was very good agreement between the B factors for the type A22 FMDV virus and empty capsid; the average B factors were 17.0 and 21.2 Å^2, respectively (Table 2).

TABLE 2. Model refinement statistics[a]

Parameter (unit)	Value
Range of spacings (Å)	24.0–3.0
Total no. of nonhydrogen atoms	5,200
No. of solvent sites	224
R_{model} (all data)[b]	20.3
ΔBonds (Å)[c]	0.017
ΔAngles (°)[d]	2.00
ΔB bonds (Å^2)[e]	2.31
ΔB angles (Å^2)[f]	3.92
Avg B (Å^2)	21.2

[a] Some 86% of residues lie in the most favored region of the Ramachandran plot, and none are in disallowed regions.

[b] $$R_{\text{model}} = \left[\frac{\sum_h |(|F_{h,obs}| - |F_{h,calc}|)|}{\sum_h |F_{h,obs}|} \right] \times 100$$

[c] Root mean square deviation from ideal covalent bond lengths.
[d] Root mean square deviation from ideal covalent bond angles.
[e] Root mean square deviation of B factors for bond restraints.
[f] Root mean square deviation of B factors for angle restraints.

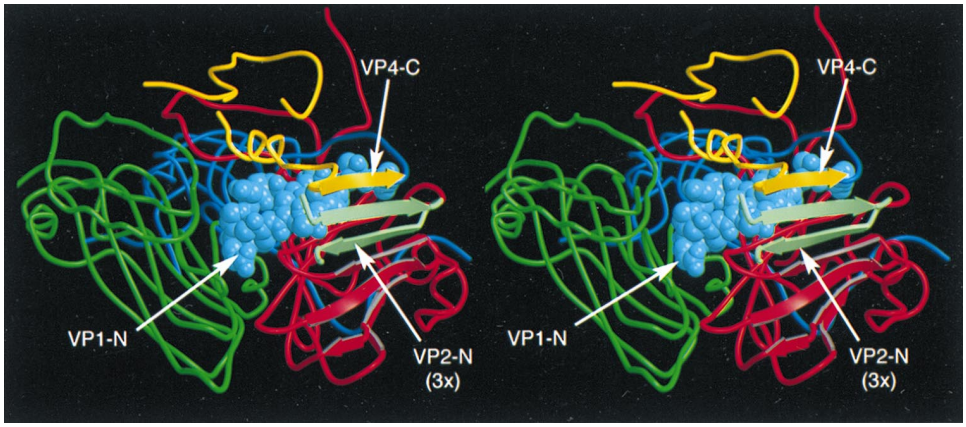

FIG. 4. The increased disordering of the N terminus of VP1 (VP1-N) and the C terminus of VP4 (VP4-C) in the empty capsid of type A22 FMDV weakens both intraprotomer and interpentamer interactions. VP1, VP2, VP3, and VP4 from a single virus protomer are shown in blue, green, red, and yellow, respectively. The atoms of the N-terminal residues of VP1, which are more disordered in the empty capsid, are represented as light blue solid spheres. These residues fill a deep cleft between VP2 and VP3 within the protomer. The mixed seven-strand β-sheet, which in the virus helps to bind together protomers from two pentamers related by threefold icosahedral symmetry, is visible on the right. The strands of the sheet are shown as flat arrows. Four strands from VP3 and one strand from VP4 are contributed by the protomer shown. Between these, in light green, are clamped two strands from the N terminus of VP2 (VP2-N) belonging to the threefold related protomer (3×; the remainder of which is not shown). In the FMDV empty capsid, the top strand of the sheet, contributed by VP4, is significantly more disordered.

DISCUSSION

Comparison of virus and empty capsid structures for FMDV. The FMDV type A22 Iraq 24/64 empty capsids used in this crystal structure determination are atypical of picornaviruses in that maturation cleavage of VP0 into VP2 and VP4, which normally occurs only upon encapsidation of viral RNA, is well advanced. The polypeptide composition of empty capsids appears to be similar to that of the mature virus, consisting of four chains rather than three.

The observed structural differences between the virus and empty capsid structures are confined to the interior of the capsid. The absence of RNA has no effect on the external surface structure, which is consistent with the antigenic identity of virus and empty capsid reported for other type A FMDVs (13, 33). There is no significant difference in the overall disposition of capsid proteins between virions and empty capsids. Thus, as has been previously observed for poliovirus (2) and canine parvovirus (37), the determinants of capsid assembly reside in capsid proteins. Nonetheless, protein-RNA interactions are likely to facilitate the initiation of assembly, explaining the observation that mature virions are usually more abundant than are empty capsids (34).

On the interior of the empty capsid, the most significant differences with the virus are found at the N terminus of VP1 and the C terminus of VP4. Although the polypeptide folds in the two structures are very similar, the B factors for these features were much higher in the empty capsid (Fig. 3), indicating that these termini are much less well ordered in the absence of packaged RNA. Thus, RNA contributes to picornavirus capsid stability by inducing protein folds that augment the interactions among proteins within the capsid.

For reasons which remain obscure, additional residues were found at the C terminus of VP4 in the empty capsid, suggesting that the VP0 precursor had been cleaved 3 residues downstream of the cleavage site observed in the mature virion. Nevertheless, this terminus adopted a fold very similar to the conformation that occurs in the virus (Fig. 2a). The conformation of the N terminus of VP1 in the empty capsid is identical to that in the virus, being pinned within a deep and predominantly hydrophobic cleft formed by the interface between VP2 and VP3 within a single protomer (Fig. 4). A combination of hydrophobic, van der Waals, and specific H-bond interactions are formed between the VP1 N terminus and the interior faces of VP2 and VP3. In the virus, these interactions may well contribute to the stability of the protomer. In the empty capsid, this stabilization is weakened by the disordering of the N terminus of VP1; a particular example of this is the loss of an H bond (conserved in other picornavirus structures) between Glu 1006 of VP1 and Ser 3154 of VP3, which appears to result in significant elevations of the B factors adjacent to the Ser residue (Fig. 3).

The interactions between protomers, particularly across interpentamer boundaries, also appear to be weaker in the empty capsid. In the virus, the C-terminal residues of VP4 (residues 4082 to 4085) and four strands of the β-barrel core of VP3 from one protomer clamp two strands belonging to the N-terminal portion of VP2 from a second protomer (Fig. 4), forming a seven-stranded β-sheet. The protomers involved in this interaction belong to different pentamers which are related by threefold icosahedral symmetry. These interactions are therefore formed only at a relatively advanced stage of capsid assembly in which pentamers of protomers come together. In empty capsids, even in the presence of VP0 cleavage to release the N terminus of VP2 and the C terminus of VP4, the relative disordering of the latter terminus clearly reduces the strength of the interpentamer association.

The coupled disordering of the C terminus of VP4 and the N terminus of VP1 in the empty capsid thus weakens both intraprotomer and interpentamer interactions. This is broadly consistent with observations that picornavirus empty capsids are generally more thermolabile than is the corresponding virion (12, 31), although the thermodynamic data are for empty capsids with intact VP0 (see below). The absence of direct RNA-protein interactions in empty capsids may also contribute to their greater thermolability, although these interactions render the FMDV virion more sensitive to acidic conditions (9).

Comparison with the structure of poliovirus empty capsids. The structure of empty capsids of poliovirus, in which VP0 is not cleaved, has previously been reported (2). The similarities and differences between the empty capsid structures for poliovirus and FMDV provide a number of insights into aspects of

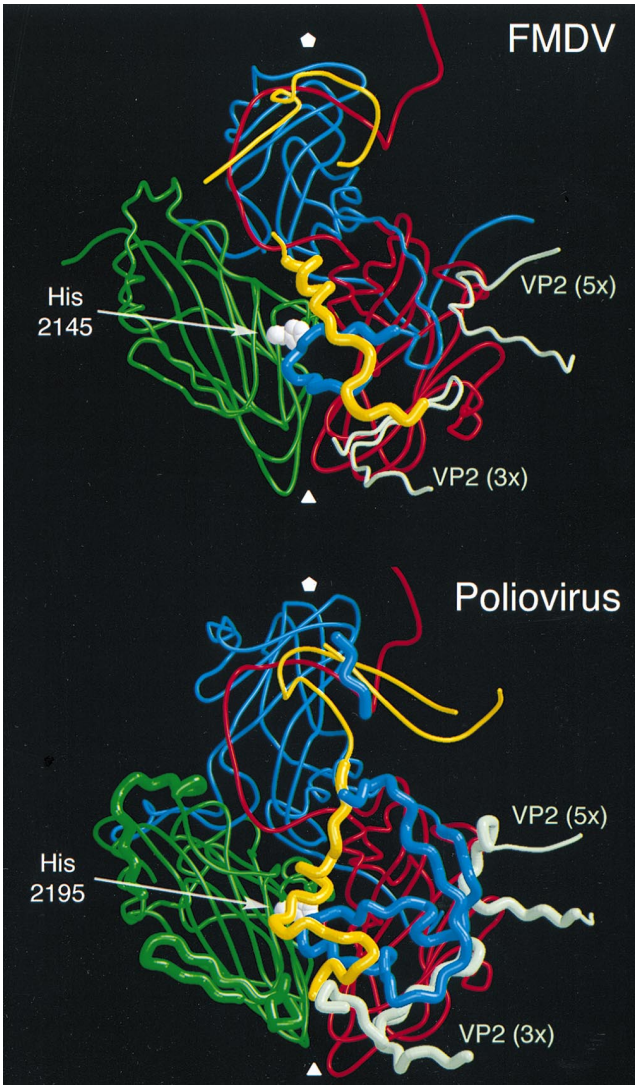

FIG. 5. Comparison of the disordering found in empty capsids of FMDV and poliovirus. In each case, a single protomer of the virus capsid is shown with VP1 to VP4 (color coded as described in the legend to Fig. 4). Additionally, two symmetry-related features of VP2 belonging to adjacent protomers are also shown in light green. The locations of the relevant three- and fivefold (3× and 5×, respectively) icosahedral symmetry axes are shown as white triangles and pentamers, respectively. Features which are disordered or rearranged in the empty capsid relative to the virus are shown as thicker tubes. On the right, residues 2039 to 2059 of VP2 from a fivefold related protomer within the same pentamer are shown. In poliovirus, this loop packs much closer to the N terminus of VP1 in the adjacent protomer than is the case in FMDV. Thus, in poliovirus empty capsids, not in FMDV empty capsids, the disordering of the VP1 N terminus appears to be coupled to the disordering of residues 2044 to 2057 of VP2. At the bottom, the N-terminal residues of VP2 from a threefold related protomer belonging to a different pentamer can be seen. These form two strands in the mixed β-sheet shown for FMDV in Fig. 4; they are ordered in FMDV but are not ordered in poliovirus. The side chain atoms of the putative catalytic histidine implicated in the cleavage of VP0, which is uncovered by the disordering of internal features in both poliovirus and FMDV empty capsids, are also shown as white spheres.

capsid stability and VP0 cleavage. As was found for FMDV, much of the difference between the virion and empty capsid structures of poliovirus is due to disordering of internal features in the empty capsid. In the poliovirus empty capsid (2), the disordered portions are residues 1001 to 1067 of VP1, residues 2014 to 2025 and 2045 to 2057 of VP2, and residues 4045 to 4056 of VP4 (Fig. 5). The N terminus of VP1 in poliovirus is extended by 42 amino acids relative to that in FMDV. Superposition of the poliovirus and FMDV structures showed that residues 1043 to 1058 in VP1 of poliovirus correspond closely to the first 16 residues at the N terminus of VP1 in FMDV. Furthermore, in poliovirus, residues 1036 to 1038 in VP1 make the β-sheet interactions which are contributed by residues 4082 to 4084 from the C terminus of VP4 in FMDV (Fig. 5). The disordering of the C terminus of VP4 and the N terminus of VP1 in FMDV empty capsids (with VP0 cleaved) mirrors the disordering of their counterparts in poliovirus (with VP0 intact).

A significant difference between the two picornaviruses is that the two β-strands from the N-terminal portion of VP2 (residues 2014 to 2026 in FMDV), which participate in a mixed seven-stranded β-sheet that holds together two protomers from different pentamers (14, 16), are ordered in FMDV empty capsids but not in poliovirus empty capsids (Fig. 5). In poliovirus empty capsids, these strands are only about 10 to 20% occupied (2). This difference may be attributed to the cleavage of VP0 in empty capsids of FMDV, which releases the N terminus of VP2 to participate in the β-sheet. In poliovirus empty capsids, the N terminus of VP2 is still covalently linked to the C terminus of VP4 and is prevented from forming β-sheet interactions. The FMDV empty capsid structure thus indicates that participation of the N terminus of VP2 in this β-sheet depends on VP0 cleavage alone, not on the presence of RNA in the capsid. Since this β-sheet helps to bind pentamers together, we would therefore expect FMDV empty capsids with VP0 intact to be less thermostable than are the capsids described here.

The two β-strands formed by the N terminus of VP2 in FMDV empty capsids with VP0 cleaved pack against residues 1017 to 1019 of VP1 from a threefold related protomer (Fig. 5). The presence of this packing interaction may help to explain why residues 1013 to 1025 in VP1 of FMDV empty capsids are relatively ordered, whereas the corresponding portion of VP1 in poliovirus empty capsids (residues 1055 to 1067) is not (2). In poliovirus, the disordering of this segment of VP1 also appears to be coupled to the disordering of residues 2045 to 2057 from VP2 in a fivefold related protomer.

Both picornavirus structures contrast with empty capsids of another small icosahedral virus, canine parvovirus. For that virus, the most significant difference between the virion and empty capsid structures is a relatively modest conformational change in a stretch of five residues that is implicated in binding to viral DNA (37).

Sequence specificity of VP0 cleavage. An unresolved question in the study of picornaviruses is the mechanism of VP0 cleavage. Early clues about this mechanism, derived from the structures of the mature virions of rhinovirus and poliovirus, ultimately proved to be misleading (18, 27). The determination of the structure of empty capsids of poliovirus has provided the basis for a new hypothesis to explain the proteolysis of VP0 (2). As noted above, although many of the internal features of capsid proteins were found to be disordered in poliovirus empty capsids, the polypeptide segment containing the scissile bond of VP0 was observed. The disordered termini revealed a hydrophobic trefoil-shaped depression on the inner surface of the capsid, centered on the icosahedral threefold axis and extending along the VP2-VP3 interface within each protomer. At the tip of this depression in each protomer, furthest from the threefold axis, was His 2195 from VP2 (Fig. 5). The peptide bond joining Asn 4069 of VP4 to Ser 2001 of VP2 within the precursor VP0 was located close to His 2195. This residue is embedded within a Pro-His-Gln motif which is conserved


a
4069
2001
Poliovirus
KTaPmLNSPNiE
FMDV
LFGALLADKKTE
4085
2001

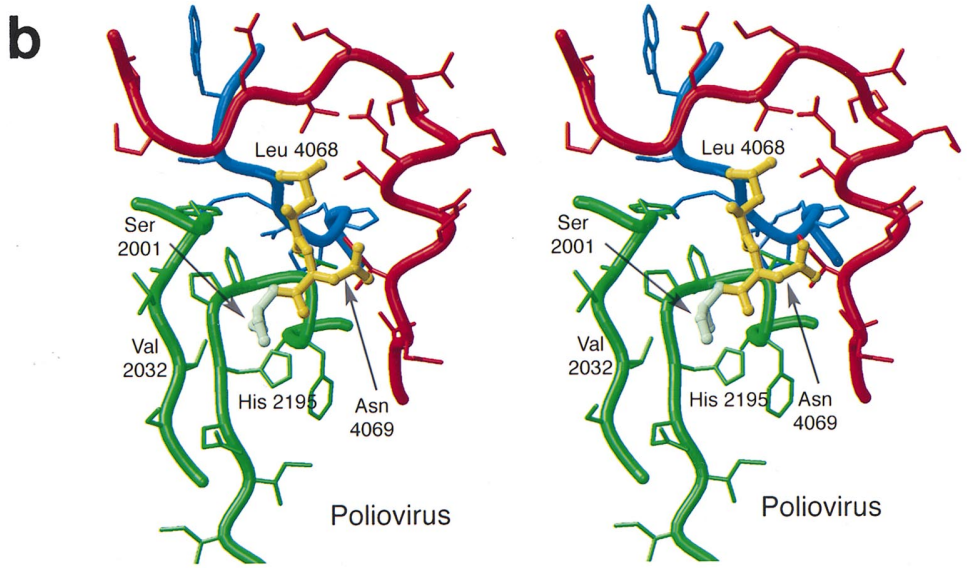
b
Leu 4068
Ser 2001
Val 2032
His 2195
Asn 4069
Poliovirus
Leu 4068
Ser 2001
Val 2032
His 2195
Asn 4069
Poliovirus

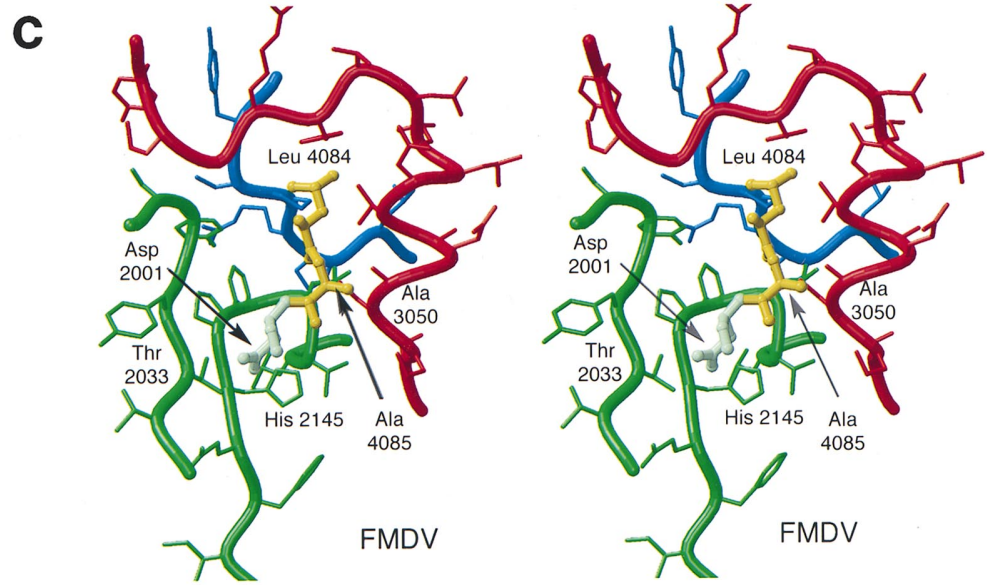
c
Leu 4084
Asp 2001
Thr 2033
Ala 3050
His 2145
Ala 4085
FMDV
Leu 4084
Asp 2001
Thr 2033
Ala 3050
His 2145
Ala 4085
FMDV

FIG. 6. Differences in the putative active sites of VP0 cleavage may account for the different substrate specificities observed for poliovirus and FMDV. (a) Comparison of the amino acid sequences in the vicinity of the scissile bond of VP0 in poliovirus and FMDV. Residues which end up in VP2 and VP4 are shown in green and yellow, respectively. Residues conserved within each genus are indicated by uppercase letters. The solid arrow shows the normal site of VP0 cleavage. The hollow arrow indicates the suggested position of aberrant cleavage observed in FMDV empty capsids. The underlined residues are present in panels b and c. (b) Putative active site at the center of the interior face of the poliovirus protomer proposed to be responsible for VP0 cleavage in poliovirus (2). Capsid proteins are shown as described in the legend to Fig. 4. The central three residues of the segment of VP0 which is cleaved during virus maturation is shown as a ball-and-stick model in the color of the capsid protein in which they ultimately reside. The side chain of Leu 4068 is bound within a hydrophobic pocket formed by contributing side chains from VP1, VP2 (VP0), and VP3. VP0 cleavage separates Asn 4069 and Ser 2001; the side chains of these residues point down onto the surface of the capsid. (c) Putative proteolytic active site on the FMDV empty capsid protomer. The N-terminal portion of VP1 and the C-terminal portion of VP4, which are disordered in the empty capsid, have been omitted. The VP0 scissile bond has been modelled within the site by applying to it the matrix operator that superposes poliovirus and FMDV empty capsids. The side chains of the residues on both sides of the scissile bond were changed by using the program O (21) to Ala 4085 and Asp 2001; for Asp 2001, a common side chain rotamer was chosen. This simple modelling exercise suggests that the principal differences between the active sites on FMDV and poliovirus account for the different amino acid specificities of the two viruses. The insertion of Ala 3050 in VP3 displaces the α-helix containing this residue toward the bound ligand; our model suggests that Ala 3050 and Ala 4085 may make a hydrophobic contact (requiring only a minimal adjustment to separate the C_β atoms to the appropriate distance). A substitution for Val 2032 in poliovirus by Thr 2033, which is rigidly conserved in FMDV, may indicate that there is a conserved hydrogen bond between the side chain of this residue and Asp 2001. Such an interaction may be required for substrate specificity. As in poliovirus, the conserved Leu which immediately precedes the residue on the carboxy-terminal side of the scissile bond is bound within a conserved hydrophobic pocket.

across all picornavirus genera (with the sole exception of hepatitis A viruses) (30). Although it remains to be determined whether the scissile bond conformation observed in poliovirus empty capsids is relevant to the cleavage process that occurs in the presence of RNA, a hypothesis that implicates His 2195 in autocatalytic cleavage of VP0 has been formulated (2). Consistent with this hypothesis and the observation that RNA encapsidation is closely linked to VP0 cleavage, it was noted that the trefoil depression is strikingly similar to a feature on the interior surface of bean pod mottle virus which has previously been shown to bind RNA (6). Although the disordering of the N terminus of VP1 and the C terminus of VP4 is less extensive (due to the premature cleavage of VP0) in the FMDV empty capsid, a similar hydrophobic depression is uncovered. In the FMDV empty capsid, as was found for poliovirus, the conserved histidine residue (His 2145 in VP2) is exposed close to the tip of this depression (Fig. 5). The correspondences between these two structures support the proposed proteolytic mechanism.

A careful examination of the putative active sites centered on the conserved histidine residues in poliovirus and FMDV provides further support for this hypothesis. There is a striking difference between the sequences in the vicinity of the VP0 scissile bonds for these two picornaviruses (Fig. 6a), and there appears to be a corresponding difference in key aspects of their active sites. In the poliovirus empty capsid structure, the side chains of both of the residues immediately flanking the scissile bond point down into the active site, with Asn 4069 directed toward a helix from VP3 (residues 3043 to 3049) and Ser 2001 directed to VP2/VP0 (Fig. 6b). Leu 4068, which is the only residue in the sequence flanking the scissile bond in VP0 that is strictly conserved across all picornavirus genera, helps to anchor the scissile bond in this conformation by binding to a conserved hydrophobic pocket (formed by the side chains of residues Pro 1271, Tyr 2035, Gly 3038, Val 3040, Glu 3045, and Leu 3046).

The scissile bond of VP0 is not present in the FMDV empty capsid structure since it has been cleaved. By superposing the two empty capsid structures, however, we produced a model that places the polypeptide segment containing the scissile bond from poliovirus VP0 within the putative proteolytic active site of FMDV (for details, see the legend to Fig. 6c). If poliovirus and FMDV do have a common mechanism of VP0 cleavage, we would expect the cleaved peptide bond to be presented to the active site in the same way in both viruses; our modelling studies indicate that this is the case. Moreover, differences in the active site of FMDV appear to be consistent with the need to recognize an Ala-Asp sequence rather than an Asn-Ser sequence. The insertion of a single residue (Ala 3050) within the α-helix of VP3 that forms one side of the pocket displaces the α-helix so that Ala 3050 is projected toward the center of the active site, where it is likely to be able to make a hydrophobic contact with Ala 4085 on the N-terminal side of the scissile bond of VP0 in FMDV (Fig. 6c). Curiously, however, a recent study found that a mutation of Ala 4085 to Asn or His in type A12 FMDV had no effect on VP0 cleavage or virus infectivity (23). It may be that these residues fit in the Ala binding pocket, satisfying the same hydrophobic contacts but with the side chain atoms beyond C_β projecting away from the interior surface of the capsid. On the opposite side of the pocket, a substitution for Val 2032 of VP2 in poliovirus with Thr 2033, which is strictly conserved in FMDV, may permit a specific H bond with the side chain of Asp 2001 on the C-terminal side of the scissile bond (VP2 numbering). Consistent with this idea, VP0 cleavage was unaffected by a conservative mutation of Asp 2001 to Asn, but a mutant containing Cys at this position was noninfectious and did not cleave VP0 (23). As in poliovirus, the conserved leucine (Leu 4084 in FMDV) secures the configuration of the cleaved peptide bond by burying itself within a conserved hydrophobic pocket (formed by residues Pro 1187, Tyr 2036, Gly 3039, Phe 3041, Asp 3046, and Val 3047, which correspond by position to those listed above for poliovirus). Thus, both the similarities and differences of the putative active sites of poliovirus and FMDV support the hypothesis of Basavappa et al. (2) for the mechanism of VP0 cleavage.

The location of the putative active-site histidine is quite intriguing. In all picornaviruses for which structures are known, it lies at the C-terminal side of the EF loop in VP2, close to the center of the protomer and at a point where components of all the major capsid proteins come together. The stretch of the VP2 polypeptide that contains the catalytic histidine makes extensive contacts with residues from the C terminus of VP1 and the N terminus of VP3 (Fig. 6). If the His residue is catalytic, its presentation in a functional context is therefore likely to be dependent on the proper folding of the entire protomer and perhaps on the assembly of the pentamer, since the C and N termini of VP1 and VP3, respectively, clearly facilitate the association of protomers into pentamers. This residue may be a structural sensor, acting to cleave VP0 only after proper assembly has occurred (and RNA encapsidation has begun). Such a mechanism would have the advantage of giving misfolded protomers a chance to refold without prematurely cleaving VP0.

ACKNOWLEDGMENTS

We thank D. Goodrich for data collection trips as disease security officer and the staff of the Synchrotron Radiation Source, Daresbury

Laboratory, for practical assistance. We are grateful to E. Ouldridge (Pittman-Moore) for the gift of infecting stocks of FMDV type A22 Iraq 24/64.

D.S. and E.F. were supported by the MRC. R.A.-G., W.B., S.C., and T.J. were supported by the BBSRC.

REFERENCES

1. **Acharya, R., E. Fry, D. Stuart, G. Fox, D. Rowlands, and F. Brown.** 1989. The three-dimensional structure of foot-and-mouth disease virus at 2.9Å resolution. Nature **337:**709–716.
1a. **Aplin, R.** Personal communication.
2. **Basavappa, R., R. Syed, O. Flore, J. P. Icenogle, D. J. Filman, and J. M. Hogle.** 1994. Role and mechanism of the maturation cleavage of VP0 in poliovirus assembly: structure of the empty capsid assembly intermediate at 2.9Å resolution. Protein Sci. **3:**1651–1669.
3. **Bishop, N. E., and D. A. Anderson.** 1993. RNA-dependent cleavage of VP0 capsid protein in provirions of hepatitis A virus. Virology **197:**616–623.
4. **Bolwell, C., A. L. Brown, P. V. Barnett, R. O. Campbell, B. E. Clarke, N. R. Parry, E. J. Ouldridge, F. Brown, and D. J. Rowlands.** 1989. Host cell selection of antigenic variants of foot-and-mouth disease virus. J. Gen. Virol. **70:**45–57.
5. **Brunger, A. T.** 1992. X-PLOR version 3.0.
6. **Chen, Z., C. Stauffacher, L. Ynge, T. Schmidt, W. Bomu, G. Kamer, M. Shanks, G. Lomonossoff, and J. E. Johnson.** 1989. Protein-RNA interactions in an icosahedral virus at 3.0Å resolution. Science **245:**154–168.
7. **Collaborative Computer Project no. 4.** 1994. The CCP4 suite: programs for protein crystallography. **D50:**760–763.
8. **Compton, S. R. B., B. Nelsen, and K. Kirkegaard.** 1990. Temperature-sensitive poliovirus mutant fails to cleave VP0 and accumulates provirions. J. Virol. **64:**4067–4075.
9. **Curry, S., C. C. Abrams, E. Fry, J. C. Crowther, G. J. Belsham, D. I. Stuart, and A. M. Q. King.** 1995. Viral RNA modulates the acid sensitivity of foot-and-mouth disease virus capsids. J. Virol. **69:**430–438.
10. **Curry, S., R. Abu-Ghazaleh, W. Blakemore, E. Fry, T. Jackson, A. King, S. Lea, D. Logan, J. Newman, and D. Stuart.** 1992. Crystallization and preliminary X-ray analysis of three serotypes of foot-and-mouth disease virus. J. Mol. Biol. **228:**1263–1268.
11. **Curry, S., E. Fry, W. Blakemore, R. Abu-Ghazaleh, T. Jackson, A. King, S. Lea, J. Newman, D. Rowlands, and D. Stuart.** 1996. Perturbations in the surface structure of A22 Iraq foot and mouth disease virus accompanying coupled changes in host cell specificity and antigenicity. Structure **4:**135–145.
12. **Doel, T. R., and P. J. Baccarini.** 1981. Thermal stability of foot-and-mouth disease virus. Arch. Virol. **70:**21–32.
13. **Doel, T. R., and W. K. T. Chong.** 1982. Comparative immunogenicity of 146S, 75S and 12S particles of foot-and-mouth disease virus. Arch. Virol. **73:**185–191.
14. **Filman, D. J., R. Syed, M. Chow, A. J. Macadam, P. D. Minor, and J. M. Hogle.** 1989. Structural factors that control conformational transitions and serotype specificity in type 3 poliovirus. EMBO J. **8:**1567–1579.
15. **Fry, E., R. Acharya, and D. Stuart.** 1993. Methods used in the structure determination of foot-and-mouth disease virus. Acta Crystallogr. **A49:**45–55.
16. **Fry, E., D. Logan, R. Acharya, G. Fox, D. Rowlands, F. Brown, and D. Stuart.** 1990. Architecture and topography of an aphthovirus. Semin. Virol. **1:**439–451.
17. **Gallagher, T. M., and R. R. Rueckert.** 1988. Assembly-dependent maturation cleavage in provirions of a small icosahedral insect ribovirus. J. Virol. **62:**3399–3406.
17a. **Grimes, J., and D. Stuart.** Unpublished program.
18. **Harber, J. J., J. Bradley, C. W. Anderson, and E. Wimmer.** 1991. Catalysis of poliovirus VP0 maturation cleavage is not mediated by serine 10 of VP2. J. Virol. **65:**326–334.
19. **Hogle, J. M., M. Chow, and D. J. Filman.** 1985. Three-dimensional structure of poliovirus at 2.9Å resolution. Science **229:**1358–1365.
20. **Jones, T. A.** 1978. Interactive computer graphics: FRODO. Methods Enzymol. **115:**157–171.
21. **Jones, T. A., J. Y. Zou, S. W. Cowan, and M. Kjeldgaard.** 1991. Improved methods for building protein models in electron density maps and the location of errors in these maps. Acta Crystallogr. **A47:**110–119.
22. **Kirchweger, R., E. Ziegler, B. J. Lamphear, D. Waters, H.-D. Liebig, W. Sommergruber, F. Sobrino, C. Hohenadl, D. Blaas, R. E. Rhoads, and T. Skern.** 1994. Foot-and-mouth disease virus leader proteinase: purification of the Lb form and determination of its cleavage site on eIF-4γ. J. Virol. **68:**5677–5684.
23. **Knipe, T., E. Rieder, B. Baxt, G. Ward, and P. W. Mason.** 1997. Characterization of synthetic foot-and-mouth disease virus provirions separates acid-mediated disassembly from infectivity. J. Virol. **71:**2851–2856.
24. **Kraulis, P. J.** 1991. MOLSCRIPT: a program to produce both detailed and schematic plots of protein structures. J. Appl. Crystallogr. **24:**946–950.
25. **Lea, S., R. Abu-Ghazaleh, W. Blakemore, S. Curry, E. Fry, T. Jackson, A. King, D. Logan, J. Newman, and D. Stuart.** 1995. Structural comparison of two strains of foot-and-mouth disease virus subtype O_1 and a laboratory antigenic variant, G67. Structure **3:**571–580.
26. **Lea, S., J. Hernandez, W. Blakemore, E. Brocchi, S. Curry, E. Domingo, E. Fry, R. Abu-Ghazaleh, A. King, J. Newman, D. Stuart, and M. G. Mateu.** 1994. The structure and antigenicity of a type C foot-and-mouth disease virus. Structure **2:**123–139.
27. **Lee, W.-M., S. S. Monroe, and R. R. Rueckert.** 1993. Role of maturation cleavage in infectivity of picornaviruses: activation of an infectosome. J. Virol. **67:**2110–2122.
27a. **Leslie, A.** Unpublished program.
28. **Luo, M., G. Vriend, G. Kamer, I. Minor, E. Arnold, M. G. Rossmann, U. Boege, D. G. Scrabe, G. M. Duke, and A. C. Palmenberg.** 1987. The atomic structure of mengo virus at 3.0Å resolution. Science **235:**182–191.
29. **Moscufo, N., A. Gomez Yafal, A. Rogove, J. M. Hogle, and M. Chow.** 1993. A mutation in VP4 defines a new step in the late stages of cell entry by poliovirus. J. Virol. **67:**5075–5078.
30. **Palmenberg, A. C.** 1989. Sequence alignments of picornaviral capsid proteins, p. 211–241. *In* B. L. Semler and E. Ehrenfeld (ed.), Molecular aspects of picornavirus infection and detection. American Society for Microbiology, Washington, D.C.
31. **Rombaut, B., K. Andries, and A. Boeyé.** 1991. A comparison of WIN 51711 and R70286 as stabilisers of poliovirus virions and procapsids. J. Gen. Virol. **72:**2153–2157.
32. **Rossmann, M. G., E. Arnold, J. W. Erickson, E. A. Frankenberger, J. P. Griffith, H.-J. Hecht, J. E. Johnson, G. Kamer, M. Luo, A. G. Mosser, R. R. Rueckert, B. Sherry, and G. Vriend.** 1985. Structure of a human common cold virus and functional relationship to other picornaviruses. Nature **317:**145–153.
33. **Rowlands, D. J., D. V. Sangar, and F. Brown.** 1975. A comparative chemical and serological study of the full and empty particles of foot-and-mouth disease virus. J. Gen. Virol. **26:**227–238.
34. **Rweyemamu, M. M., G. Terry, and T. W. F. Pay.** 1979. Stability and immunogenicity of empty particles of foot-and-mouth disease virus. Arch. Virol. **59:**69–79.
35. **Ryan, M. D., G. J. Belsham, and A. M. Q. King.** 1989. Specificity of enzyme-substrate interactions in foot-and-mouth disease virus polyprotein processing. Virology **173:**35–45.
36. **Stuart, D.** 1994. Virus structure—docking mission accomplished. Nature **371:**19–20.
37. **Wu, H., and M. G. Rossmann.** 1993. The canine parvovirus empty capsid structure. J. Mol. Biol. **233:**231–244.